Dynamical Disorder of π-Molecular Structures Induced by Proton Dynamics in an Organic Ferroelectric Compound

J. Fujioka,[1] S. Horiuchi,[2] F. Kagawa,[3] and Y. Tokura[1,2,3,4]

[1]*Department of Applied Physics, University of Tokyo, Tokyo 113-8656, Japan*
[2]*National Institute of Advanced Industrial Science and Technology (AIST), Tsukuba 305-8562, Japan*
[3]*Multiferroics Project, ERATO, Japan Science and Technology Corporation, Tokyo 113-8656, Japan*
[4]*Cross-Correlated Materials Research Group (CMRG), RIKEN Advanced Science Institute, Wako 351-0198, Japan*

(Received 21 November 2008; published 12 May 2009)

We have investigated the optical response resulting from the proton-π-electron-molecular-skeleton coupled dynamics in an organic ferroelectric 55DMBP-Hia. Upon the ferroelectric-to-paraelectric transition, almost all of the vibrational modes below 500 cm^{-1} are anomalously blurred and amalgamated into the high-frequency tail of the polarization-relaxation mode. This indicates that the constituent molecular shape is no more well defined around T_C due to the dynamical disorder of the π-conjugated structure originating from proton delocalization on the intermolecular bifurcated hydrogen bond.

DOI: 10.1103/PhysRevLett.102.197601 PACS numbers: 78.30.Jw, 77.22.−d, 77.84.Fa

Strongly correlated proton dynamics in a variety of materials with the hydrogen-bond network causes versatile phase transition phenomena and relevant changes in electronic and structural properties [1]. Ferroelectricity as observed in KH_2PO_4 (KDP) and its analogs is one example and has been the issue of extensive investigations for several decades [2]. For these materials, the interplay among the proton, charge, and lattice degrees of freedom plays a crucial role in the emergence of the spontaneous polarization concomitant with the proton ordering. Recently, a new class of room-temperature hydrogen-bond ferroelectrics has been developed in the family of organic molecular solids and is now of great interest in light of emerging organic electronics [3]. In those, the constituent molecules are interconnected with the hydrogen bond, and the collective intermolecular proton transfer induces the electric polarization concomitant with the asymmetric molecular distortion via the strong proton-π-molecular-skeleton correlation. In addition, the form of the hydrogen bond is unprecedented among hydrogen-bonded ferroelectrics; the proton is shared by three surrounding atoms due to the bifurcated hydrogen bond. In this Letter, we report on the anomalous dynamical disorder of the molecular structures observed around the ferroelectric transition temperature in such a molecular ferroelectric, which may arise from the proton-mediated strong coupling between the polarization relaxation and the molecular-skeleton shape dynamics.

The prototypical example is a recently synthesized cocrystal of 5, 5′-dimethyl-2, 2′-bipyridine (55DMBP) and iodanilic acid (Hia) [4]. In 55DMBP-Hia, alternately arranged molecules of Hia and 55DMBP form one-dimensional hydrogen-bond chains along the $2c$-b axis, as schematically shown in Fig. 1(a). Each molecule is stacked with the π-electron overlap in individual columns parallel to the b axis. At the ground state, one of the two protons in Hia is transferred to 55DMBP via the hydrogen bonds; the protons are alternately localized either on an oxygen (O) atom of the Hia moiety or on a nitrogen (N) atom of the 55DMBP one, as shown in Fig. 1(a). This proton order and the concurrent asymmetric molecular distortion give rise to the spontaneous polarization along the hydrogen-bond chain. At $T_c = 269$ K, the ferroelectric-to-paraelectric transition occurs accompanying the melting of the proton order. In the paraelectric phase, the proton is disordered within every intermolecular O . . . N bond and the Hia molecule restores the inversion symmetry on a time average. The possible changes of the

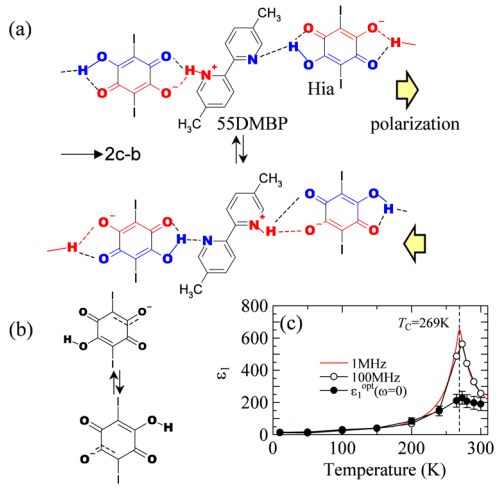

FIG. 1 (color online). (a) The schematic view of the polar hydrogen-bond chain and its reversal for 55DMBP-Hia. The blue and red (online) parts are protonated or deprotonated π-conjugated fragments, respectively. (b) The resonance structure of Hia at the paraelectric phase. (c) The temperature dependence of the dielectric constant ϵ_1 along the hydrogen-bond chain ($2c$-b axis) at 1 and 100 MHz as well as $\epsilon_1^{opt}(\omega = 0)$ (see text).

 © 2009 The American Physical Society

π-conjugated structures of Hia are shown in Fig. 1(b) [4]. The temperature (T) dependence of the dielectric constant at 1 MHz ($\epsilon_1^{1\,\mathrm{MHz}}$) for $E \parallel 2c\text{-}b$ is reproduced in Fig. 1(c). $\epsilon_1^{1\,\mathrm{MHz}}$ for $E \parallel 2c\text{-}b$ exhibits a divergent behavior at T_c and is as large as 300 at room temperature. This is contrasted with $\epsilon_1^{1\,\mathrm{MHz}}$ for $E \parallel a$ and $E \parallel b$ (not shown), which yields a much smaller value ($\leq$10) with minimal T dependence. As already shown for the existing hydrogen-bonding ferroelectrics such as KH_2PO_4 (KDP) [5–7], the optical excitations in the infrared frequency range play a crucial role in the ferroelectric transition and the related dielectric anomaly concomitant with the melting of the proton order. In the hydrogen-bonding organic ferroelectrics, furthermore, there may emerge the strong coupling of the correlated proton dynamics with the molecular π electrons and skeletons, which should manifest itself in the low-energy and molecular-vibrational optical spectra. In this work, we have investigated the T dependence of the infrared-optical spectra for 55DMBP-Hia to reveal the roles of the proton dynamics in the coupled fluctuation of the polarization and molecular skeleton and discussed the origin of the dielectric anomaly in the course of the ferroelectric transition.

Single crystals of 55DMBP-Hia were prepared by the slow-evaporation method, details of which have been reported elsewhere [4]. The reflectivity spectra were measured in the frequency range of 30–40 000 cm^{-1}. Spectra of the real and imaginary parts of the dielectric constant (ϵ_1 and ϵ_2) were calculated by the Kramers-Kronig analysis. For the analysis, we assumed a constant reflectivity below 30 cm^{-1} and ω^{-4} extrapolation above 40 000 cm^{-1}.

We show the T dependence of the reflectivity spectra for $E \parallel 2c\text{-}b$ (hydrogen-bond chain direction) in Fig. 2(a). At 10 K, the sharp peaks originating from the molecular vibrations are observed below 1700 cm^{-1}. As T increases, the peaks below 500 cm^{-1} are rapidly blurred, and a high reflectance band reminiscent of the soft mode shows up below 110 cm^{-1}. On the contrary, the intensity of each vibrational peak is much smaller for $E \parallel b$ than for $E \parallel 2c\text{-}b$ as shown in Fig. 2(b). Henceforth, we focus on the spectra for $E \parallel 2c\text{-}b$.

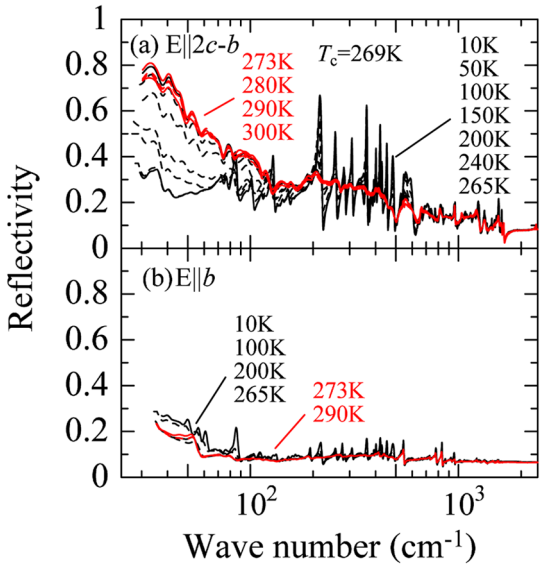

FIG. 2 (color online). Reflectivity spectra of 55DMBP-Hia for (a) $E \parallel 2c\text{-}b$ and (b) $E \parallel b$ at various temperatures.

In Fig. 3(a), we plot the ϵ_2 spectra in the frequency range of 1530–1670 cm^{-1}. The three peaks at 1560, 1610, and 1650 cm^{-1} observed at 300 K are assigned to the monovalent C-O (C-O$^-$), C═C, and C═O stretching mode in the Hia moiety, respectively. The subsistence of the C-O$^-$ stretching mode at $T > T_c$ indicates that the Hia molecule is ionic even in the paraelectric phase [4,8]. As T decreases, the C═O stretching mode splits into the double-peak structure denoted as C═O$_a$ and C═O$_b$ at $T < T_c$, while the intensity of the C-O$^-$ and C═C stretching mode monotonically increases. The splitting of the C═O stretching modes can be attributed to the nonequivalent two C═O bonds of the Hia moiety in the ferroelectric phase; one of the two π-conjugated fragments corresponding to the enol form of a β-diketone (HO-C═C—C═O) is protonated, and another is deprotonated as shown in Fig. 1(a). According to the conventional mechanism of the motional narrowing, the competition between the mode splitting and

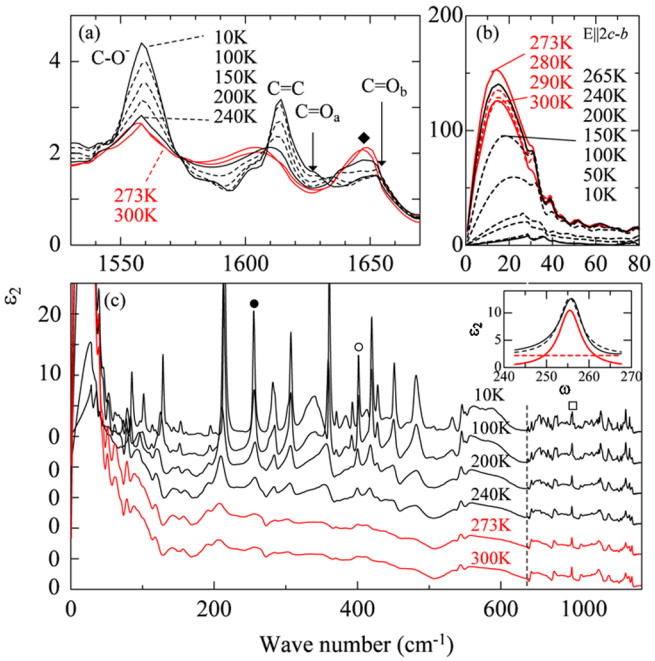

FIG. 3 (color online). Spectra of the imaginary part of dielectric constant ϵ_2 in the frequency range of (a) 1530–1670, (b) 0–80, and (c) 0–1800 cm^{-1}. The closed diamond in (a) and closed and open circle and open square in (c) indicate the 1650, 255, 403, and 976 cm^{-1} mode of the Hia moiety, respectively (see also text). In the frequency range of 640–1800 cm^{-1}, the spectra are plotted on a logarithmic scale of wave number. In (c), the ordinate base line is successively shifted for clarity. The inset shows the fitting results for the 255 cm^{-1} mode at 100 K. The thin solid and dashed lines correspond to the experimental and fitted curve, respectively. The thick solid and dashed lines correspond to the first and second term in Eq. (1), respectively.

the fluctuation frequency determines the persistence or amalgamation of the two modes [9]; the rapid fluctuation with a higher frequency than the mode splitting promotes the amalgamation of the double-peak structure. The emergence of the broad- but single-peak feature at a frequency in between those of the C═O_a and C═O_b [marked with a closed diamond in Fig. 3(a)] indicates that the proton fluctuation is enhanced to a comparable frequency scale with the original mode splitting (25 cm^{-1}) as T increases toward T_C [10]. This frequency scale can be well compared with that of the polarization fluctuation mode closely coupled with the proton dynamics, as argued in the following.

We show the ϵ_2 spectra below 80 cm^{-1} in Fig. 3(b). While the spectral weight below 40 cm^{-1} is minimal at 10 K, it increases with increasing T toward T_C, leading to the formation of the broad band centered at ~20 cm^{-1}. With further increase of T above T_c, the spectral intensity appears to be slightly reduced. To see the contribution of this band to the dc dielectric constant, we plot the T dependence of the ϵ_1 spectra extrapolated to zero frequency [$\epsilon_1^{\rm opt}(\omega = 0)$] in Fig. 1(c) as well as that of $\epsilon_1^{1\,\rm MHz}$ and $\epsilon_1^{100\,\rm MHz}$. Although the discrepancy between $\epsilon_1^{\rm opt}(\omega = 0)$ and $\epsilon_1^{1\,\rm MHz}$ or $\epsilon_1^{100\,\rm MHz}$ is still appreciable around T_C, the optical excitation at ~20 cm^{-1} significantly contributes to the enhancement of the dc dielectric constant [11]. Such a T evolution of this band may be related with the enhancement of the proton fluctuation (~25 cm^{-1}) as probed by the spectral shape of the C═O stretching mode. In KDP, a similar low-frequency optical excitation is observed for the $E \parallel P$ spectra around T_C and is attributed to the relaxation mode of the PO_4 electric dipoles coupled with the proton fluctuation [5–7]. By analogy with KDP, the optical excitation around 20 cm^{-1} in this organic ferroelectric may be assigned to the polarization-relaxation mode coupled to the proton-π-molecular-skeleton dynamics.

In Fig. 3(c), we show the T dependence of the ϵ_2 spectra in the frequency range of 0–1800 cm^{-1}. At 10 K, many molecular-vibrational modes are observed over a wide frequency range. It is worth noting that all of the peaks below 500 cm^{-1} begin to be dramatically blurred in return for the evolution of the polarization-relaxation mode with increasing T. These peaks are assigned to the modes having a large contribution from the C═O, C-O, C-I, and ring-bending motion of the Hia moiety or those from the ring-bending motion of the 55DMBP moiety [12,13]. For example, the peaks at 255 and 403 cm^{-1} [denoted with closed and open circles in Fig. 3(c), respectively] are assigned to the in-plane ring-bending mode coupled to the C-I stretching, C-I bending, and C-O bending motion and that coupled to the C-O bending, C-C stretching, and C═O bending motion in the Hia moiety, respectively. By contrast, several modes having a large contribution from the C═O, C-O, C-I, C═C, and C-C stretching motion in the Hia moiety above 500 cm^{-1} are not significantly blurred as T increases. For example, the peak at 976 cm^{-1}, which is denoted with an open square in Fig. 3(c) and assigned to the C-C stretching mode coupled to the C-I bending and C-O stretching motion in the Hia moiety, remains to be clearly observed even at $T > T_C$. To quantitatively discuss the relation between the disappearance of each vibrational mode and the evolution of the polarization-relaxation mode, we fitted these three modes in terms of the Lorentz oscillator model

$$\epsilon_2(\omega) = \frac{S\omega_0^2\gamma\omega}{(\omega^2 - \omega_0^2)^2 + \omega_0^2\gamma^2} + \epsilon_2^{\rm rlx}. \quad (1)$$

Here S is the oscillator strength, ω_0 the mode frequency, and γ the damping rate. $\epsilon_2^{\rm rlx}$ is the fitting parameter for the contribution from the T-dependent broad continuum, i.e., the tail of the polarization-relaxation mode at ω_0, and assumed ω-independent in the fitting procedure near ω_0. The example of the fitting for 255 cm^{-1} mode is demonstrated in the inset in Fig. 3(c). We identify the T dependence of the spectral weight ($S\omega_0^2$), γ, and $\epsilon_2^{\rm rlx}$ by defining $\Delta S\omega_0^2 = S\omega_0^2(T) - S\omega_0^2(300\ {\rm K})$, $\Delta\gamma = \gamma(T)/\gamma(10\ {\rm K})$, and $\Delta\epsilon_2^{\rm rlx} = \epsilon_2^{\rm rlx}(T) - \epsilon_2^{\rm rlx}(10\ {\rm K})$, respectively. In Fig. 4(a), we show the T dependence of $\Delta\epsilon_2^{\rm rlx}$ as well as that of $\Delta\epsilon_2$ at 20 cm^{-1} as a measure of the evolution of the polarization-relaxation mode. $\Delta\epsilon_2^{\rm rlx}$ for the 255 and 403 cm^{-1} modes increases as T increases toward T_C, reflecting the evolution of the polarization-relaxation mode. By contrast, $\Delta\epsilon_2^{\rm rlx}$ for the 976 cm^{-1} mode shows minimal T dependence, indicating that the tail of the polarization-relaxation mode is no longer appreciable at

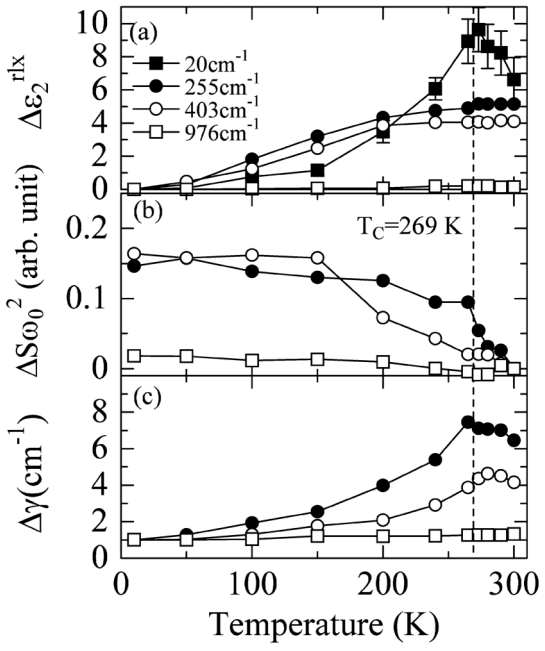

FIG. 4. The temperature dependence of (a) $\Delta\epsilon_2^{\rm rlx}$, (b) $\Delta S\omega_0^2$, and (c) $\Delta\gamma$ for the 255, 403, and 976 cm^{-1} mode is shown by closed and open circles and open squares, respectively (see also text). Closed squares in (a) are ϵ_2 ($\times 1/15$) at 20 cm^{-1}.

such a high frequency. We plot $\Delta S\omega_0^2$ and $\Delta\gamma$ for each mode as a function of T in Figs. 4(b) and 4(c), respectively. $\Delta S\omega_0^2$ ($\Delta\gamma$) for the 255 and 403 cm^{-1} modes decreases (increases) as T increases toward T_C, while that for the 976 cm^{-1} mode is much less T-dependent. This indicates that the time scale of the proton fluctuation, which is typically $\sim$20 cm^{-1}, extensively distributes up to as rapid as $\sim$500 cm^{-1}, and hence each discrete vibrational mode, which strongly interacts with the continuum via the proton-molecular-skeleton correlation, is no longer well defined at the paraelectric phase.

Such a transformation of almost all of the vibrational modes into the polarization-relaxation mode in such a wide frequency range has never been observed for the conventional proton-π-electron coupled dielectrics such as the squaric acid to the best of our knowledge [14]. The unconventionally large and rapid proton-π-molecular-skeleton fluctuation in the present ferroelectric may originate from the special hydrogen-bonding form as characterized in the following. As seen in Fig. 1(a), the Hia molecule contains two β-diketone fragments linked to each other with significantly short O...O distance (d_{OO}) due to the strong resonance-assisted hydrogen bond, which promotes the proton and π-electron delocalization in the Hia molecule ($^{-}$O-C═C—C═O ⇔ O═C—C═C—O^{-}) [15]. In addition, O atoms in these fragments are connected to N atom in the 55DMBP moiety with a short O...N distance, forming the intermolecular bifurcated hydrogen bond (two O atoms and one N atom). Recently, Horiuchi *et al.* revealed that the protonation or deprotonation process significantly modifies the bond angles as well as the bond length in both the Hia and 55DMBP moiety; the molecular distortion is closely tied to the proton location [4]. Thus, the dynamical proton disorder over the two O- and one N-bonded sites may strongly enhance the fluctuation of the π-electron-molecular-skeleton coupled system. In the conventional hydrogen-bonded dielectrics such as the squaric acid crystal, the proton motion between the double-well minima is slow enough for the molecular-vibrational motion to be well defined even at the paraelectric phase [14]. This is not the case for the present system; the effective proton potential minima should be shallow and broad due to the intermolecular bifurcated hydrogen bond [4,16]. Thus, it is anticipated that the rapid proton fluctuation due to the intermolecular bifurcated hydrogen bond and the strong proton-π-molecular-skeleton correlation are responsible for the large π-electron-molecular-skeleton coupled fluctuation, leading to the drastic transformation of the discrete vibrational modes into the polarization-relaxation mode in a wide frequency range below 500 cm^{-1}.

In summary, we have investigated the infrared-optical spectra for the organic hydrogen-bonded ferroelectric 55DMBP-Hia with the focus on the π-electron-molecular-skeleton dynamics strongly tied with the intermolecular proton fluctuation. Around T_C, almost all of the vibrational modes below 500 cm^{-1} are significantly blurred and amalgamated into the underlying polarization-relaxation mode. This signals the dynamical disorder or strong fluctuation of the π-molecular structure originating from the proton delocalization on the intermolecular bifurcated hydrogen bond, which may characterize this emerging family of room-temperature hydrogen-bonded molecular ferroelectrics.

This work was in part supported by Grant-In-Aid for Scientific Research (No. 20110003) by the Ministry of Education, Culture, Sports, Science and Technology of Japan.

[1] G. A. Jeffery, *An Introduction to Hydrogen Bonding* (Oxford University Press, Oxford, 1997).
[2] M. E. Lines and A. M. Glass, *Principles and Applications of Ferroelectrics and Related Materials* (Oxford University Press, New York, 1977).
[3] S. Horiuchi and Y. Tokura, Nature Mater. **7**, 357 (2008).
[4] S. Horiuchi, R. Kumai, and Y. Tokura, Angew. Chem., Int. Ed. **46**, 3497 (2007).
[5] P. Simon, F. Gervais, and E. Courtens, Phys. Rev. B **37**, 1969 (1988).
[6] S. Shin *et al.*, J. Phys. Soc. Jpn. **63**, 2612 (1994).
[7] Y. Tominaga, H. Urabe, and M. Tokunaga, Solid State Commun. **48**, 265 (1983).
[8] According to the recent neutron diffraction measurements, the Hia is nominally monovalent at $T < T_C$, while it takes an intermediate structure between ionic and neutral at $T > T_C$.
[9] A. Abragam, *The Principles of Nuclear Magnetism* (Clarendon Press, Oxford, 1962).
[10] The reason why the amalgamated band is not at the mean position of C═O_a and C═O_b may be the difference in probability of the protonated or deprotonated configurations of the π-conjugated fragment at the paraelectric phase, as revealed by a recent neutron diffraction study [R. Kumai *et al.* (to be published)].
[11] One possible explanation may be the presence of the lower frequency optical excitation such as the domain wall dynamics, which cannot be captured by the present experiment. In general, such a low-frequency domain wall dynamics also significantly contributes to the dc dielectric constant as well as the polarization-relaxation mode.
[12] A. Pawlukojc *et al.*, J. Phys. Org. Chem. **16**, 709 (2003).
[13] L. Ould-Moussa *et al.*, J. Raman Spectrosc. **31**, 377 (2000).
[14] Y. Moritomo, S. Koshihara, and Y. Tokura, J. Chem. Phys. **93**, 5429 (1990).
[15] G. Gilli, F. Bellucci, V. Ferretti, and V. Bertolasi, J. Am. Chem. Soc. **111**, 1023 (1989).
[16] R. Kumai, S. Horiuchi, Y. Okimoto, and Y. Tokura, J. Chem. Phys. **125**, 084715 (2006).